JOURNAL OF COMPUTATIONAL PHYSICS **127,** 73–87 (1996)
ARTICLE NO. 0159

Symmetry-Breaking and Bifurcation Study on the Laminar Flows through Curved Pipes with a Circular Cross Section*

ZHONG-HUA YANG† AND RUI-SONG YE‡

†*Department of Mathematics, Shanghai University of Science and Technology, Shanghai, 201800, China;* ‡*Institute of Mathematics, Shantou University, Guangdong, 515063, China*

Received January 31, 1995; revised January 24, 1996

The Dean problem of steady viscous flow through a coiled circular pipe is studied numerically. We compute the structure of the symmetric families of the flows that exist as the crucial parameter D varies, which is in accordance with those stated in Yang and Keller (*Appl. Numer. Math.* **2,** 257, 1986). Furthermore, we find a asymmetric flow emanating from the symmetry-breaking bifurcation point, which they could not find since they restricted the numerical study on the flows symmetric about the x-axis. © 1996 Academic Press, Inc.

1. INTRODUCTION

The flow through curved pipes has long been studied since the early works of Dean [4, 5]. For example, Dennis [6], Collins and Dennis [2], and Dennis and Ng [7] have computed such flows when the coiling ratio a/L is small. Here a is the pipe radius and L is the radius of the curvature of the axis of the pipe. Van Dyke [10] has applied the Stoke series and the Dombes–Sykes technique to this problem. Yang and Keller [13] have computed the structure of the symmetric families of the steady, laminar, viscous flows through a curved pipe of circular cross section that exists as the crucial parameter D varies. Here D is the Dean number defined by

$$D \equiv Ga^3(2a/L)^{1/2}/(\mu\nu),$$

where G is the constant pressure gradient driving the flow, μ is the viscosity, and ν is the coefficient of kinematic viscosity.

For the pipe with a rectangular cross section, Winters [12] has computed the bifurcation structure of the flows and found that a pair of asymmetric solutions arise from a symmetry-breaking bifurcation point on the primary symmetric flow branch.

Daskopoulos and Lenhoff [3] have shown that for the case of the circular cross solution the two- and four-vortex symmetric solutions are stable to symmetric disturbances, while the symmetric branch joining them is unstable. They pointed out that there were unresolved issues including the possibility of asymmetric solutions and the response to asymmetric disturbances and the effects of curvature.

In this paper, we would like to solve the above issues proposed by Daskopoulos and Lenhoff [3]. We are interested in finding the asymmetric solution branch after the symmetry-breaking bifurcation takes place for the flow of the pipe with a circular cross section. Thus, we should make Fourier expansions of the stream function, axial velocity, and vorticity in more complete forms (3.1), which means that the unknown Fourier coefficients are doubled and the nonlinear terms in the equations are more complicated. Meanwhile the stability of the solution branches of the flows to asymmetric disturbances and the effects of curvature are also considered.

The outline of the paper will be as follows. In Section 2 we formulate the problem, retaining the exact equations (valid to all orders in $\varepsilon = a/L$) which means that we consider the effects of axial curvature. Expansions in Fourier series are introduced in Section 3 to get a system of the Fourier coefficients. Numerical methods are introduced in Section 4. These employ centered difference and Newton's methods with continuation and path following techniques introduced by Keller [9]. The stability of the flows to asymmetric disturbances is also discussed in Section 4. The extended systems which are used to locate the fold point and the symmetry-breaking bifurcation point accurately, are proposed in Section 5. Numerical results are presented and discussed in Section 6.

2. GENERAL FORMULATION

We employ the notation used in [2, 7] as indicated in Fig. 1. The circular cross section of the tube in the (x, y)-plane has radius a with the centre at L on the x-axis. The tube is coiled about a circle of radius L in the (x, z)-plane. With no pitch in the coil the tube thus forms a torus. Our equations are exact for this case. Dimensionless velocity components of the fluid are (u, v, w) at a point P with

* This work was supported by NSFC and State Major Key Project for Basic Research.

0021-9991/96 $18.00
Copyright © 1996 by Academic Press, Inc.
All rights of reproduction in any form reserved.

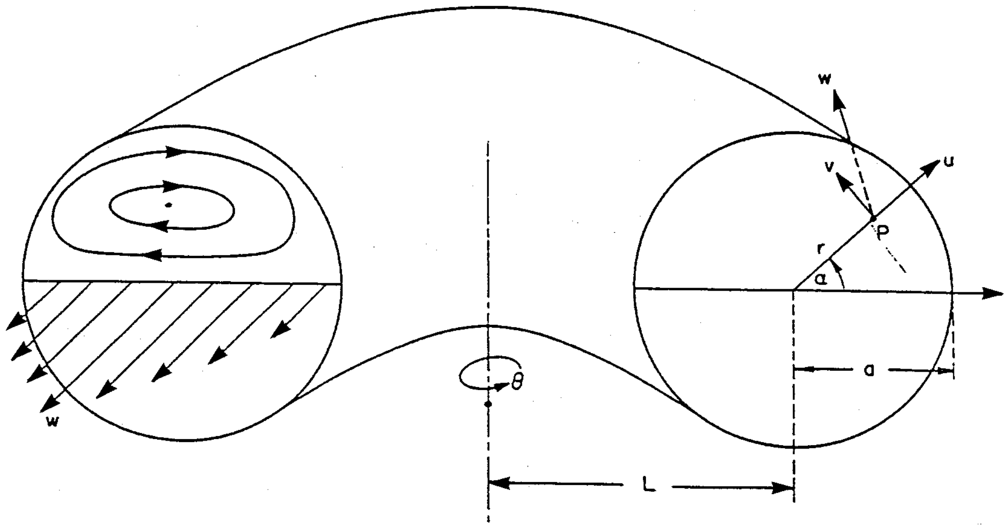

FIG. 1. The tube cross sections showing coordinates, velocity components, axial flow distribution sketch and cross-flow streamlines sketch.

dimensionless polar coordinates (r, α). Here u is the radial part and v is the angular section and $r \equiv r'/a$, where r' is the dimensional radius.

We seek flows independent of θ, the angular deviation from the (x, y)-plane. A stream function $\phi(r, \alpha)$ is introduced in terms of which the transverse velocity components are given by

$$u(r, \alpha) = \frac{1}{r(1 + \varepsilon r \cos \alpha)} \frac{\partial \phi}{\partial \alpha}, \qquad v(r, \alpha) = \frac{-1}{(1 + \varepsilon r \cos \alpha)} \frac{\partial \phi}{\partial r}. \tag{2.1}$$

Here $\varepsilon \equiv \alpha/L$ is the "coiling ratio" and the continuity equation is thus satisfied. Using these velocity components in the Navier–Stokes equations we introduce the modified Laplacian

$$\tilde{\nabla}^2 \equiv \frac{1 + \varepsilon r \cos \alpha}{r} \left[\frac{\partial}{\partial r} \left(\frac{r}{1 + \varepsilon r \cos \alpha} \frac{\partial}{\partial r} \right) + \frac{1}{r} \frac{\partial}{\partial \alpha} \left(\frac{1}{1 + \varepsilon r \cos \alpha} \frac{\partial}{\partial \alpha} \right) \right] \tag{2.2}$$

and the vorticity

$$\Omega = -\tilde{\nabla}^2 \phi, \tag{2.3}$$

to get for the w-momentum equation,

$$\tilde{\nabla}^2 w + \frac{1}{r(1 + \varepsilon r \cos \alpha)} \left(\frac{\partial \phi}{\partial r} \frac{\partial w}{\partial \alpha} - \frac{\partial \phi}{\partial \alpha} \frac{\partial w}{\partial r} \right) = -D, \tag{2.4}$$

and, on elimination of the pressure from the other momentum equation,

$$\tilde{\nabla}^2 \Omega + \frac{1}{r(1 + \varepsilon r \cos \alpha)} \left(\frac{\partial \phi}{\partial r} \frac{\partial \Omega}{\partial \alpha} - \frac{\partial \phi}{\partial \alpha} \frac{\partial \Omega}{\partial r} \right) + \frac{2\varepsilon \Omega}{(1 + \varepsilon r \cos \alpha)^2} \left(\sin \alpha \frac{\partial \phi}{\partial r} + \frac{\cos \alpha}{r} \frac{\partial \phi}{\partial \alpha} \right) = \frac{w}{(1 + \varepsilon r \cos \alpha)^2} \left(\sin \alpha \frac{\partial w}{\partial r} + \frac{\cos \alpha}{r} \frac{\partial w}{\partial \alpha} \right). \tag{2.5}$$

Boundary conditions on the wall of the tube, $r = 1$, yield

$$w(1, \alpha) = \phi(1, \alpha) = \frac{\partial \phi}{\partial r}(1, \alpha) = 0, \quad 0 \le \alpha \le \pi. \tag{2.6}$$

Let the problem (2.3)–(2.5) be rewritten as the operator form,

$$G(Z, D, \varepsilon) = 0, \tag{2.7}$$

where $Z = (\Omega, w, \phi)$. Obviously, the problem (2.3)–(2.5) is Z_2-symmetric, i.e.,

$$SG(Z, D, \varepsilon) = G(SZ, D, \varepsilon),$$

where $SZ(r, \alpha) = (-\Omega(r, -\alpha), w(r, -\alpha), -\phi(r, -\alpha))$.

Yang and Keller [13] only studied the symmetric flows, that is, they assumed

$$w(r, -\alpha) = w(r, \alpha), \quad \phi(r, -\alpha) = -\phi(r, \alpha), \quad \Omega(r, -\alpha) = -\Omega(r, \alpha). \tag{2.8}$$

But in this paper we do not assume (2.8), as a result, both of the symmetric and the asymmetric solution branches are expected.

3. FOURIER SERIES EXPANSIONS

To solve the boundary value problem posed in (2.2)–(2.6) we seek Fourier expansions of the stream function, the axial velocity, and the vorticity in the forms:

$$\phi(r,\alpha) = \sum_{k=1}^{\infty} f_k(r)\sin k\alpha + \sum_{k=0}^{\infty} h_k(r)\cos k\alpha; \quad (3.1a)$$

$$w(r,\alpha) = \sum_{k=1}^{\infty} u_k(r)\sin k\alpha + \sum_{k=0}^{\infty} w_k(r)\cos k\alpha; \quad (3.1b)$$

$$\Omega(r,\alpha) = \sum_{k=1}^{\infty} g_k(r)\sin k\alpha + \sum_{k=0}^{\infty} v_k(r)\cos k\alpha. \quad (3.1c)$$

Using the expansions (3.1) in the differential equations (2.3)–(2.5) and applying the orthogonality properties and other identities for the trigonometric functions yields an infinite system of coupled nonlinear, second-order ordinary differential equations for the coefficient functions $\{f_k(r), g_k(r), u_k(r), h_k(r), v_k(r), w_k(r)\}$. Specifically, we get from (2.3), with $f_0(r) \equiv g_0(r) \equiv 0$, $h_{-1}(r) \equiv v_{-1}(r) \equiv 0$:

$$\frac{1}{2}\varepsilon r\left[\frac{d^2}{dr^2} - \frac{(k-1)(k-2)}{r^2}\right] f_{k-1}(r) + \left[\frac{d^2}{dr^2} + \frac{1}{r}\frac{d}{dr} - \frac{k^2}{r^2}\right] f_k(r) + \frac{1}{2}\varepsilon r\left[\frac{d^2}{dr^2} - \frac{(k+1)(k+2)}{r^2}\right] f_{k+1}(r)$$
$$= -\frac{1}{2}\varepsilon r g_{k-1}(r) - g_k(r) - \frac{1}{2}\varepsilon r\, g_{k+1}(r), \quad k \geq 1; \quad (3.2a)$$

$$\frac{1}{2}\varepsilon r(1+\delta_{k,1})\left[\frac{d^2}{dr^2} - \frac{(k-1)(k-2)}{r^2}\right] h_{k-1}(r) + \left[\frac{d^2}{dr^2} + \frac{1}{r}\frac{d}{dr} - \frac{k^2}{r^2}\right] h_k(r) + \frac{1}{2}\varepsilon r\left[\frac{d^2}{dr^2} - \frac{(k+1)(k+2)}{r^2}\right] h_{k+1}(r)$$
$$= -\frac{1}{2}(1+\delta_{k,1}(r)\varepsilon r v_{k-1}(r) - v_k(r) - \frac{1}{2}\varepsilon r v_{k+1}(r), k \geq 0. \quad (3.2b)$$

From (2.4), we obtain, with $u_0(r) \equiv 0$, $w_{-1}(r) \equiv 0$:

$$\frac{1}{2}\varepsilon r(1+\delta_{k,1})\left[\frac{d^2}{dr^2} - \frac{(k-1)(k-2)}{r^2}\right] w_{k-1}(r) + \left[\frac{d^2}{dr^2} + \frac{1}{r}\frac{d}{dr} - \frac{k^2}{r^2}\right] w_k(r) + \frac{1}{2}\varepsilon r \left[\frac{d^2}{dr^2} - \frac{(k+1)(k+2)}{r^2}\right] w_{k+1}(r) = R_{1k}(r)$$
$$+ R_{3k}(r) - \delta_{k,1}\varepsilon r D - \delta_{k,0} D, \quad k \geq 0; \quad (3.3a)$$

$$\frac{1}{2}\varepsilon r\left[\frac{d^2}{dr^2} - \frac{(k-1)(k-2)}{r^2}\right] u_{k-1}(r) + \left[\frac{d^2}{dr^2} + \frac{1}{r}\frac{d}{dr} - \frac{k^2}{r^2}\right] u_k(r) + \frac{1}{2}\varepsilon r\left[\frac{d^2}{dr^2} - \frac{(k+1)(k+2)}{r^2}\right]$$
$$u_{k+1}(r) = R_{2k}(r) + R_{4k}(r), \quad k \geq 1. \quad (3.3b)$$

From (2.5) we get, with $g_{-1}(r) \equiv g_0(r) \equiv 0$, $v_{-1}(r) \equiv 0$:

$$\left(\frac{1}{2}\varepsilon r\right)^2\left[\frac{d^2}{dr^2} - \frac{(k-2)(k-3)}{r^2}\right] g_{k-2}(r) + \frac{1}{2}\varepsilon r\left[2\frac{d^2}{dr^2} + \frac{1}{r}\frac{d}{dr} - \frac{(k-1)(2k-3)}{r^2}\right] g_{k-1}(r)$$
$$+ \left\{\left[\frac{d^2}{dr^2} + \frac{1}{r}\frac{d}{dr} - \frac{k^2}{r^2}\right] + \frac{1}{2}\varepsilon^2 r^2\left[\frac{d^2}{dr^2} - \frac{k^2}{r^2}\right]\right\} g_k(r)$$
$$- \delta_{k,1}\left(\frac{\varepsilon^2 r^2}{4}\frac{d^2}{dr^2} - \frac{\varepsilon^2}{2}\right) g_k(r) + \frac{1}{2}\varepsilon r\left[2\frac{d^2}{dr^2} + \frac{1}{r}\frac{d}{dr} - \frac{(k+1)(2k+3)}{r^2}\right] g_{k+1}(r) + \left(\frac{1}{2}\varepsilon r\right)^2\left[\frac{d^2}{dr^2} - \frac{(k+2)(k+3)}{r^2}\right] g_{k+2}(r) = \frac{1}{2}\varepsilon r N_{k-1}(r) + N_k(r)$$
$$+ \frac{1}{2}\varepsilon r N_{k+1}(r) + P_{1k}(r) + \frac{1}{2}\varepsilon Q_{1k}(r), \quad k \geq 1; \quad (3.4a)$$

$$\left(\frac{1}{2}\varepsilon r\right)^2 (1+\delta_{k,2})\left[\frac{d^2}{dr^2} - \frac{(k-2)(k-3)}{r^2}\right] v_{k-2}(r) + \frac{1}{2}\varepsilon r(1+\delta_{k,1})\left[2\frac{d^2}{dr^2} + \frac{1}{r}\frac{d}{dr} - \frac{(k-1)(2k-3)}{r^2}\right] v_{k-1}(r)$$
$$+ \left\{\left[\frac{d^2}{dr^2} + \frac{1}{r}\frac{d}{dr} - \frac{k^2}{r^2}\right] + \frac{1}{2}\varepsilon^2 r^2\left[\frac{d^2}{dr^2} - \frac{k^2}{r^2}\right]\right\} v_k(r)$$
$$- \delta_{k,1}\left(\frac{\varepsilon^2 r^2}{4}\frac{d^2}{dr^2} - \frac{\varepsilon^2}{2}\right) v_k(r) + \frac{1}{2}\varepsilon r\left[2\frac{d^2}{dr^2} + \frac{1}{r}\frac{d}{dr} - \frac{(k+1)(2k+3)}{r^2}\right] v_{k+1}(r) + \left(\frac{1}{2}\varepsilon r\right)^2\left[\frac{d^2}{dr^2} - \frac{(k+2)(k+3)}{r^2}\right] v_{k+2}(r) = \frac{1}{2}\varepsilon r M_{k-1}(r) + M_k(r)$$
$$+ \frac{1}{2}\varepsilon r M_{k+1}(r) + P_{2k}(r) + \frac{1}{2}\varepsilon Q_{2k}(r), \quad k \geq 0; \quad (3.4b)$$

where $\delta_{k,j}$ is the Kronecker symbol and R_{1k}, R_{2k}, R_{3k}, R_{4k}, P_{1k}, P_{2k}, Q_{1k}, Q_{2k}, M_k, N_k are defined as follows:

$$R_{1k}(r) \equiv \frac{(1+\delta_{k,0})^{-1}}{2r} \sum_{n=0}^{\infty} \{[|n-k| f_{|n-k|}(r) + (n+k) f_{n+k}(r)] w_n'(r) + n\,[f'_{n+k}(r) + \operatorname{sign}(n-k) f'_{|n-k|}(r)] w_n(r)\}; \tag{3.5a}$$

$$R_{3k}(r) \equiv -\frac{(1+\delta_{k,0})^{-1}}{2r} \sum_{n=0}^{\infty} \{[|n-k| u_{|n-k|}(r) + (n+k) u_{n+k}(r)] h_n'(r) + n[u'_{n+k}(r) + \operatorname{sign}(n-k) u'_{|n-k|}(r)] h_n(r)\}; \tag{3.5b}$$

$$R_{2k}(r) \equiv \frac{1}{2r} \sum_{n=1}^{\infty} \{[|n-k| f_{|n-k|}(r) - (n+k) f_{n+k}(r)] u_n'(r) - n[f'_{n+k}(r) - \operatorname{sign}(n-k) f'_{|n-k|}(r)] u_n(r)\}; \tag{3.6a}$$

$$R_{4k}(r) \equiv \frac{1}{2r} \sum_{n=0}^{\infty} \{[(n-k) h_{|n-k|}(r) - (n+k) h_{n+k}(r)] w_n'(r) - n[(1+\delta_{n-k} h'_{|n-k|}(r) + h'_{n+k}(r)] w_n(r)\}; \tag{3.6b}$$

$$N_k(r) \equiv \frac{1}{2r} \left\{ \sum_{n=1}^{\infty} \{[|n-k| f_{|n-k|}(r) - (n+k) f_{n+k}(r)] g_n'(r) - n[f'_{n+k}(r) - \operatorname{sign}(n-k) f'_{|n-k|}(r)] g_k(r)\} + \sum_{n=0}^{\infty} \{[(n-k) h_{|n-k|}(r) - (n+k) h_{n+k}(r)] v_n'(r) + n\,[-f'_{n+k}(r) + (1+\delta_{n,k}) h'_{|n-k|}(r)] v_k(r)\} \right\}; \tag{3.7}$$

$$M_k(r) \equiv \frac{(1+\delta_{k,0})^{-1}}{2r} \left\{ \sum_{n=0}^{\infty} \{[|n-k| f_{|n-k|}(r) + (n+k) f_{n+k}(r)] v_n'(r) + n[f'_{n+k}(r) + \operatorname{sign}(n-k) f'_{|n-k|}(r)] v_k(r)\} + \sum_{n=1}^{\infty} \{[(k-n) h_{|n-k|}(r) - (n+k) h_{n+k}(r)] g_n'(r) - n[h'_{n+k}(r) + (1+\delta_{n,k}) h'_{|n-k|}(r)] g_k(r)\} \right\}; \tag{3.8}$$

$$P_{1k}(r) \equiv \frac{1}{4} \left\{ \sum_{n=0}^{\infty} \{w_n'(r) - \frac{n}{r} w_n(r)][(1+\delta_{k,n+1}) w_{|n+1-k|}(r) - w_{n+1+k}(r)] - [w_n'(r) + \frac{n}{r} w_n(r)][(1+\delta_{n-1,k}) w_{|n-1-k|}(r) - (1+\delta_{n+k,1}) w_{n-1+k}(r)]\} + \sum_{n=1}^{\infty} \left\{ \left[u_n'(r) - \frac{n}{r} u_n(r) \right] [-u_{n+k+1}(r) + \operatorname{sign}(n+1-k) u_{|n+1-k|}(r)] + \left[u_n'(r) + \frac{n}{r} u_n(r) \right] [u_{n-1+k}(r) - \operatorname{sign}(n-1-k) u_{|n-1-k|}(r)]\} \right\}; \tag{3.9}$$

$$P_{2k}(r) \equiv \frac{(1+\delta_{k,0})^{-1}}{4} \left\{ \sum_{n=1}^{\infty} \left\{ u_n'(r) - \frac{n}{r} u_n(r) \right] [-(1+\delta_{k,n+1}) w_{|n+1-k|}(r) - w_{n+1+k}(r)] + \left[u_n'(r) + \frac{n}{r} u_n(r) \right] [(1+\delta_{n-1,k}) w_{|n-1-k|}(r) + (1+\delta_{n+k,1}) w_{n-1+k}(r)] \right\} + \sum_{n=0}^{\infty} \left\{ \left[w_n'(r) - \frac{n}{r} w_n(r) \right] [u_{n+k+1}(r) + \operatorname{sign}(n+1-k) u_{|n+1-k|}(r)] + \left[w_n'(r) + \frac{n}{r} w_n(r) \right] [-\operatorname{sign}(n-1+k) u_{|n-1+k|}(r) - \operatorname{sign}(n-1-k) u_{|n-1-k|}(r)] \right\} \right\}; \tag{3.10}$$

$$Q_{1k}(r) \equiv \sum_{n=1}^{\infty} \left\{ \left[f_n'(r) - \frac{n}{r} f_n(r) \right] [g_{n+k+1}(r) - \operatorname{sign}(n+1-k) g_{|n+1-k|}(r)] - \left[f_n'(r) + \frac{n}{r} f_n(r) \right] [g_{n-1+k}(r) - \operatorname{sign}(n-1-k) g_{|n-1-k|}(r)] \right\} + \sum_{n=0}^{\infty} \left\{ h_n'(r) - \frac{n}{r} h_n(r) \right] [-(1+\delta_{k,n+1}) v_{|n+1-k|}(r) + v_{n+1+k}(r)] - \left[h_n'(r) + \frac{n}{r} h_n(r) \right] [-(1+\delta_{n-1,k}) v_{|n-1-k|}(r) + (1+\delta_{n+k,1}) v_{n-1+k}(r)] \right\} \right\}; \tag{3.11}$$

$$Q_{2k}(r) \equiv (1 + \delta_{k,0})^{-1}\left\{\sum_{n=0}^{\infty}\left\{\left[h_n'(r) - \frac{n}{r}h_n(r)\right][-g_{n+k+1}(r) - \text{sign}(n+1-k)g_{|n+1-k|}(r)] + \left[h_n'(r) + \frac{n}{r}h_n(r)\right][\text{sign}(n-1+k)g_{|n-1+k|}(r) + \text{sign}(n-1-k)g_{|n-1-k|}(r)]\right\} + \left\{\sum_{n=1}^{\infty}\left\{f_n'(r) - \frac{n}{r}f_n(r)\right][(1+\delta_{k,n+1})v_{|n+1-k|}(r) + v_{n+1+k}(r)] - \left[f_n'(r) + \frac{n}{r}f_n(r)\right][(1+\delta_{n-1,k})v_{|n-1-k|}(r) + (1+\delta_{n+k,1})v_{n-1+k}(r)]\right\}. \quad (3.12)$$

At the origin, $r = 0$, of the polar coordinates (r, α) continuity requires that $\phi(0, \alpha)$, $w(0, \alpha)$, $\Omega(0, \alpha)$ be independent of α. From (3.1) we thus obtain that

$$f_k(0) = h_k(0) = w_k(0) = u_k(0) = g_k(0) = v_k(0) = 0, \quad k = 1, 2, \ldots. \quad (3.13a)$$

For simplicity we assume that

$$h_0(0) = v_0(0) = 0. \quad (3.13b)$$

Note that a condition on $w_0(0)$ is not obtained, but $w_0(0) = w(0, \alpha)$. The condition (2.6) at $r = 1$ applied to (3.1a) (3.1b) yields

$$f_k(1) = 0, \quad k \geq 1, \quad (3.14a)$$

$$f_k'(1) = 0, \quad k \geq 1, \quad (3.14b)$$

$$h_k(1) = 0, \quad k \geq 0, \quad (3.14c)$$

$$h_k'(1) = 0, \quad k \geq 0, \quad (3.14d)$$

$$w_k(1) = 0, \quad k \geq 0, \quad (3.14.e)$$

$$u_k(1) = 0, \quad k \geq 1. \quad (3.14f)$$

The formal consistency of the "order" of the system and the number of boundary conditions seems to be off by one, since all of the equations are second order and we do not have two boundary conditions on $w_0(r)$. This is easily remedied by noting that the equation in (3.3) for $k = 0$ can be reduced to a first-order equation. To do this we multiply by r and integrate over $[0, r]$. In evaluating at $r = 0$ we use (3.13) and the assumption that

$$\lim_{r\to 0}[rw_0'(r)] = \lim_{r\to 0}[r^2 w_1'(r)] = 0;$$

the result is the first-order equation

$$\frac{d}{dr}w_0(r) + \frac{1}{2}\varepsilon r\left[\frac{d}{dr}w_1(r) - \frac{2}{r}w_1(r)\right] = \frac{1}{2r}\sum_{n=1}^{\infty}(nf_n(r)w_n(r) - nh_n(r)u_n(r)) - \frac{1}{2}rD. \quad (3.15)$$

The analytical problem is thus reduced to solving (3.2a) for $k \geq 1$, (3.2b) for $k \geq 0$, (3.3a) for $k \geq 1$, (3.3b) for $k \geq 1$, (3.4a) for $k \geq 1$, (3.4b) for $k \geq 0$, and (3.15) subject to the boundary conditions (3.13) and (3.14).

4. NUMERICAL PROCEDURES

To solve, or rather to approximate, the solution of the problem formulated in Section 3 we first truncate the Fourier expansions, then we use difference approximations on the system of ODEs, and finally solve the nonlinear difference equations by means of Newton's method and continuation procedures. We describe these techniques below.

4.1. *Truncation of the Fourier Expansions*

Under the assumption that the series in (3.1) converge sufficiently rapidly we replace them by the finite trigonometric expansions obtained by setting

$$f_k(r) \equiv h_k(r) \equiv g_k(r) \equiv v_k(r) \equiv w_k(r) \equiv u_k(r) \equiv 0, \quad k > K. \quad (4.1a)$$

We then use (4.1a) in the Eqs. (3.2)–(3.15) and obtain a system of $6K + 2$ second-order and one first-order ordinary differential equations for the $6K + 3$ unknowns,

$$\begin{aligned} &f_k(r), g_k(r), u_k(r), \quad 1 \leq k \leq K; \\ &h_k(r), v_k(r), w_k(r), \quad 0 \leq k \leq K. \end{aligned} \quad (4.1b)$$

There are $12K + 5$ boundary conditions in (3.13) and (3.14) when we terminate those relations at $k = K$. We seek to solve this two-point boundary value problem numerically.

4.2. *Differential Approximations*

We replace a uniform grid of points $r_j = jh$, $0 \leq j \leq M + 1$, with $r_{M+1} = 1$ on the interval $0 \leq r \leq 1$. At each point of the grid we introduce approximations to the coefficients in (4.1b) with the notation

$$\begin{aligned} &f_k(r_j) \doteq f_{k,j}, \quad h_k(r_j) \doteq h_{k,j}, \quad g_k(r_j) \doteq g_{k,j}, \\ &v_k(r_j) \doteq v_{k,j}, \quad u_k(r_j) \doteq u_{k,j}, \quad w_k(r_j) \doteq w_{k,j}. \end{aligned}$$

We employ the difference operators, for any mesh function, say u_j:

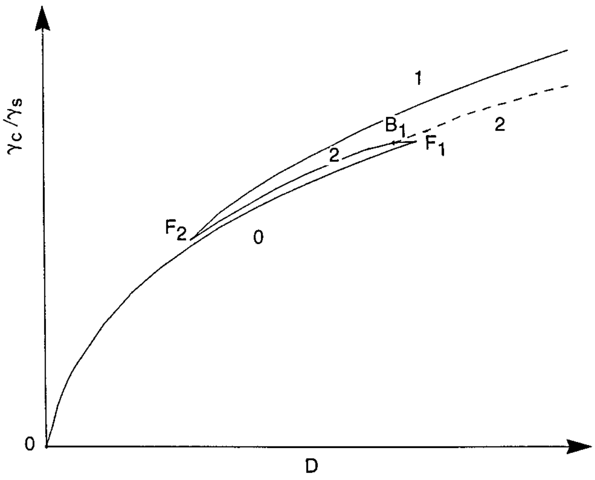

FIG. 2. Stability results: the figures Mp on the branches denote the number of positive eigenvalues of Jacobian $G_X(X; D, \varepsilon)$: —, symmetric solutions; ---, asymmetric solutions.

$$D_+ u_j \equiv \frac{u_{j+1} - u_j}{h}, \quad D_- u_j \equiv \frac{u_j - u_{j-1}}{h}, \quad D_0 u_j \equiv \frac{u_{j+1} - u_{j-1}}{2h}.$$

Then the discrete or difference approximations to (3.2), (3.3), and (3.4) are taken to be

$$\frac{1}{2}\varepsilon r_j \left[D_+ D_- - \frac{(k-1)(k-2)}{r_j^2}\right] f_{k-1,j} + \left[D_+ D_- + \frac{1}{r_j} D_0 - \frac{k^2}{r_j^2}\right] f_{k,j} + \frac{1}{2}\varepsilon r_j \left[D_+ D_- - \frac{(k+1)(k+2)}{r_j^2}\right] f_{k+1,j} = -\frac{1}{2}\varepsilon r_j g_{k-1,j} - g_{k,j} - \frac{1}{2}\varepsilon r_j g_{k+1,j}, \quad k \geq 1; \tag{4.2a}$$

$$\frac{1}{2}\varepsilon r_j (1 + \delta_{k,1}) \left[D_+ D_- - \frac{(k-1)(k-2)}{r_j^2}\right] h_{k-1,j} + \left[D_+ D_- + \frac{1}{r_j} D_0 - \frac{k^2}{r_j^2}\right] h_{k,j} + \frac{1}{2}\varepsilon r_j \left[D_+ D_- - \frac{(k+1)(k+2)}{r_j^2}\right] h_{k+1,j} = -\frac{1}{2}\varepsilon r_j (1 + \delta_{k,1}) v_{k-1,j} - v_{k,j} - \frac{1}{2}\varepsilon r_j v_{k+1,j}, \quad k \geq 0; \tag{4.2b}$$

$$\frac{1}{2}\varepsilon r_j (1 + \delta_{k,1}) \left[D_+ D_- - \frac{(k-1)(k-2)}{r_j^2}\right] w_{k-1,j} + \left[D_+ D_- + \frac{1}{r_j} D_0 - \frac{k^2}{r_j^2}\right] w_{k,j} + \frac{1}{2}\varepsilon r_j \left[D_+ D_- - \frac{(k+1)(k+2)}{r_j^2}\right] w_{k+1,j} = R_{1k,j} + R_{3k,j} - \delta_{k,1}\, \varepsilon r_j D - \delta_{k,0} D, \quad k \geq 0; \tag{4.3a}$$

$$\frac{1}{2}\varepsilon r_j \left[D_+ D_- - \frac{(k-1)(k-2)}{r_j^2}\right] u_{k-1,j} + \left[D_+ D_- + \frac{1}{r_j} D_0 - \frac{k^2}{r_j^2}\right] u_{k,j} + \frac{1}{2}\varepsilon r_j \left[D_+ D_- - \frac{(k+1)(k+2)}{r_j^2}\right] u_{k+1,j} = R_{2k,j} + R_{4k,j}, \quad k \geq 1; \tag{4.3b}$$

$$\left(\frac{1}{2}\varepsilon r_j\right)^2 \left[D_+ D_- - \frac{(k-2)(k-3)}{r_j^2}\right] g_{k-2,j} + \frac{1}{2}\varepsilon r_j \left[2D_+ D_- + \frac{1}{r_j} D_0 - \frac{(k-1)(2k-3)}{r_j^2}\right] g_{k-1,j} + \left\{\left[D_+ D_- + \frac{1}{r_j} D_0 - \frac{k^2}{r_j^2}\right] + \frac{1}{2}\varepsilon^2 r_j^2 \left[D_+ D_- - \frac{k^2}{r_j^2}\right]\right\} g_{k,j} - \delta_{k,1}\left(\frac{1}{4}\varepsilon^2 r_j^2 D_+ D_- - \frac{\varepsilon^2}{2}\right) g_{k,j} + \frac{1}{2}\varepsilon r_j \left[2D_+ D_- + \frac{1}{r_j} D_0 - \frac{(k+1)(2k+3)}{r_j^2}\right] g_{k+1,j} + \left(\frac{1}{2}\varepsilon r_j\right)^2 \left[D_+ D_- - \frac{(k+2)(k+3)}{r_j^2}\right] g_{k+2,j} = \frac{1}{2}\varepsilon r_j N_{k-1,j} + N_{k,j} + \frac{1}{2}\varepsilon r_j N_{k+1,j} + P_{1k,j} + \frac{1}{2}\varepsilon Q_{1k,j}, \quad k \geq 1; \tag{4.4a}$$

$$\left(\frac{1}{2}\varepsilon r_j\right)^2 (1 + \delta_{k,2}) \left[D_+ D_- - \frac{(k-2)(k-3)}{r_j^2}\right] v_{k-2,j} + \frac{1}{2}\varepsilon r_j (1 + \delta_{k,1}) \left[2D_+ D_- + \frac{1}{r_j} D_0 - \frac{(k-1)(2k-3)}{r_j^2}\right] v_{k-1,j} + \left\{\left[D_+ D_- + \frac{1}{r_j} D_0 - \frac{k^2}{r_j^2}\right] + \frac{1}{2}\varepsilon^2 r_j^2 \left[D_+ D_- - \frac{k^2}{r_j^2}\right]\right\} v_{k,j} - \delta_{k,1}\left(\frac{\varepsilon^2 r_j^2}{4} D_+ D_- - \frac{\varepsilon^2}{2}\right) v_{k,j} + \frac{1}{2}\varepsilon r_j \left[2D_+ D_- + \frac{1}{r_j} D_0\right.$$

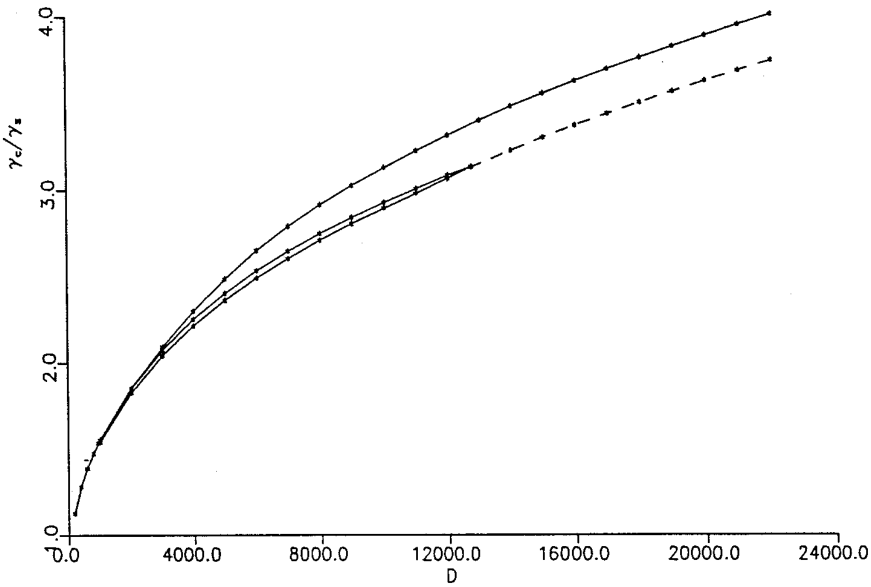

FIG. 3. Friction ratio, γ_c/γ_s, vs. Dean number, D, for case $k = 10$, $h = \frac{1}{40}$, $\varepsilon = 0.0$.

$$- \frac{(k+1)(2k+3)}{r_j^2}\Bigg] v_{k+1,j} + \left(\frac{1}{2}\varepsilon r_j\right)^2 \Bigg[D_+ D_- - \frac{(k+2)(k+3)}{r_j^2}\Bigg] v_{k+2,j} = \frac{1}{2}\varepsilon r_j M_{k-1,j} + M_{k,j} + \frac{1}{2}\varepsilon r_j M_{k+1,j} + P_{2k,j} + \frac{1}{2}\varepsilon Q_{2k,j}, \quad k \geq 0. \tag{4.4b}$$

Each of these difference equations is imposed for $j = 1, 2, \ldots, M$. The quantities $R_{1k,j}$, $R_{2k,j}$, $R_{3k,j}$, $R_{4k,j}$, $N_{k,j}$, $M_{k,j}$, $P_{1k,j}$, $P_{2k,j}$, $Q_{1k,j}$, and $Q_{2k,j}$ are the obvious finite difference approximations to the quantities in (3.5)–(3.12) centered at r_j. Since only first derivatives occur in these expressions we employ $D_0 f_{n,j}$ to approximate $f'_n(r_j)$, etc. The remaining first-order equation (3.15) is centered at the points $r_{j-1/2} \equiv (j - \frac{1}{2})h$ as

$$D_- w_{0,j} + \frac{1}{2}\varepsilon r_{j-1/2}[D_- w_{1,j} - (2/r_{j-1/2})\frac{1}{2}(w_{1,j} + w_{1,j-1})]$$

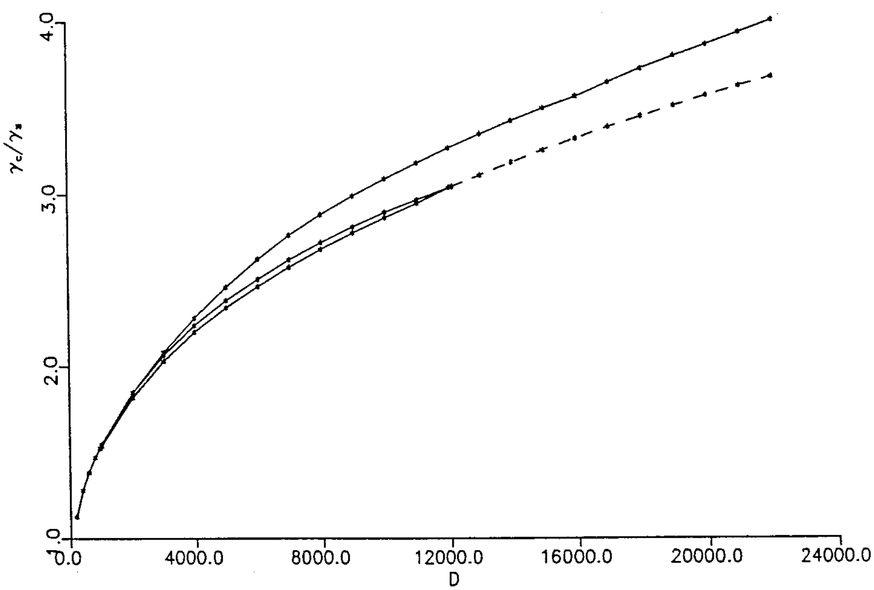

FIG. 4. Friction ratio, γ_c/γ_s, vs Dean number, D, for case $k = 15$, $h = \frac{1}{40}$, $\varepsilon = 0.0$.

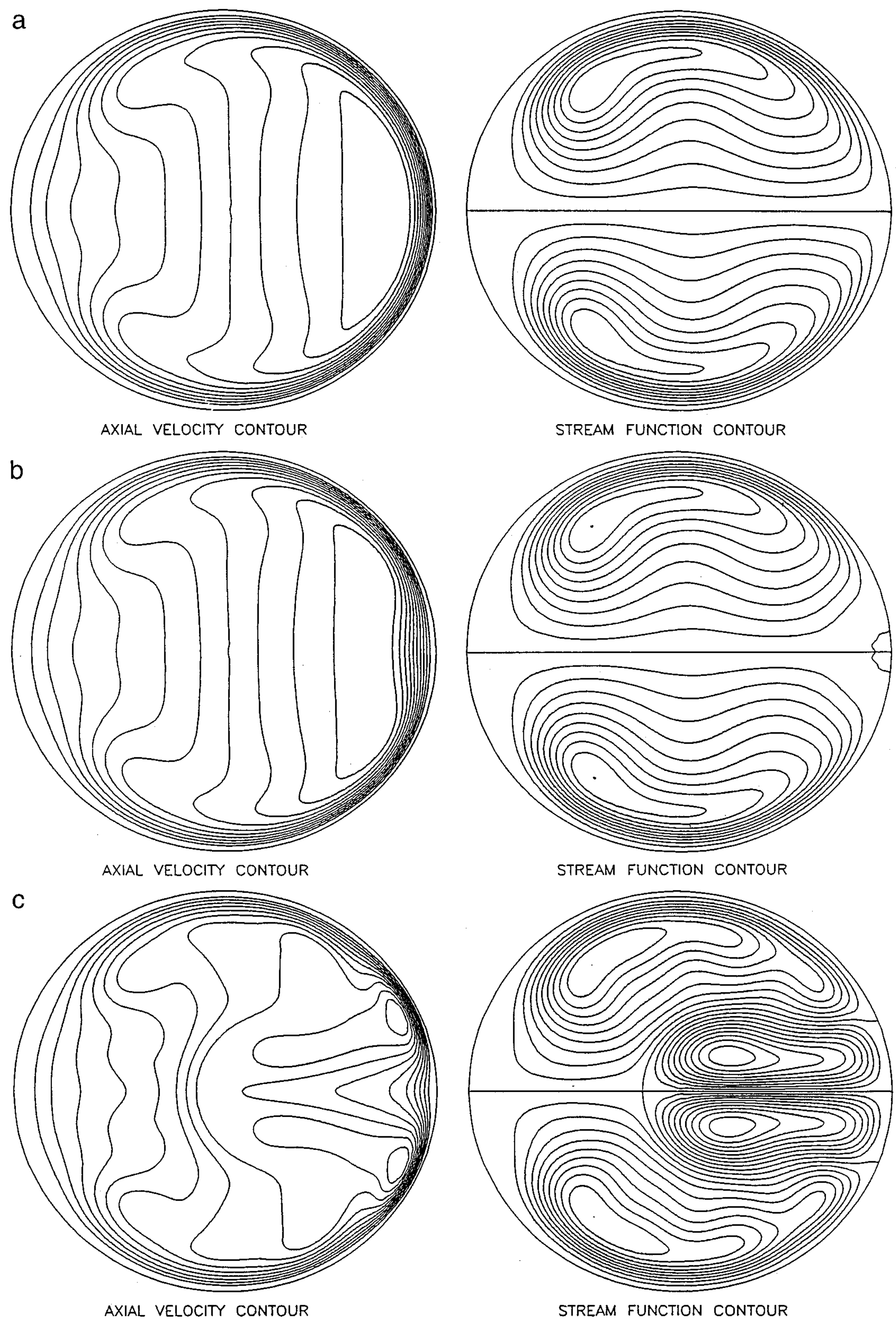

FIG. 5. Axial velocity, w, and stream function, ϕ, contour lines: $D = 8000$, $K = 10$, $h = \frac{1}{40}$, $\varepsilon = 0$. (a) First symmetric branch: Max $w = 618.4$, Min $w = 0$, Max $\phi = 24.08$, Min $\phi = -24.08$. (b) Second symmetric branch: Max $w = 628.9$, Min $w = 0$, Max $\phi = 23.04$, Min $\phi = -23.04$. (c) Third symmetric branch: Max $w = 601.3$, Min $w = 0$, Max $\phi = 21.76$, Min $\phi = -21.76$. (d) $D = 18000$. Asymmetric branch: Max $w = 1102$, Min $w = 0$, Max $\phi = 32.51$, Min $\phi = -32.51$.

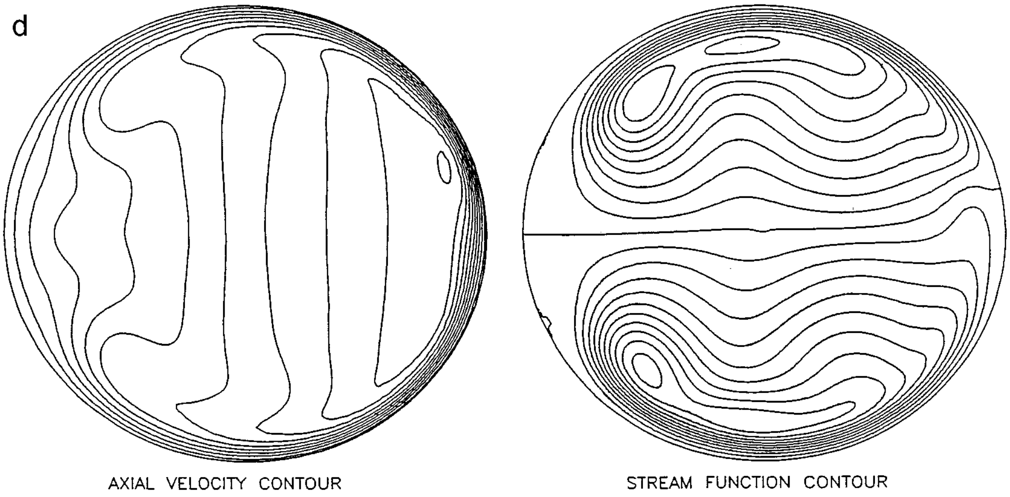

FIG. 5—*Continued*

$$= \frac{1}{2r_{j-1/2}} \sum_{n=1}^{K} \left[n \frac{1}{2}(f_{n,j} + f_{n,j-1}) \frac{1}{2}(w_{n,j} + w_{n,j-1}) - n \frac{1}{2}(h_{n,j} + h_{n,j-1}) \frac{1}{2}(u_{n,j} + u_{n,j-1}) \right] - r_{j-1/2} \frac{1}{2} D, \quad j = 1, 2, ..., M+1. \tag{4.5}$$

The boundary conditions (3.13) and (3.14) become the corresponding conditions:

$$f_{k,0} = h_{k,0} = g_{k,0} = v_{k,0} = w_{k,0} = u_{k,0} = 0, \quad k = 1, 2, ..., K;$$
$$h_{0,0} = 0; v_{0,0} = 0; \tag{4.6a}$$
$$f_{k,M+1} = h_{k,M+1} = w_{k,M+1} = u_{k,M+1} = 0, \quad k = 1, 2, ..., K;$$
$$h_{0,M+1} = w_{0,M+1} = 0. \tag{4.6b}$$

The remaining conditions, in (3.14b), (3.14d), are imposed in order to retain second-order accuracy as

$$D_0 f_{k,M+1} \equiv \frac{f_{k,M+2} - f_{k,M}}{2h} = 0, \quad k = 1, 2, ..., K;$$
$$D_0 h_{k,M+1} \equiv \frac{h_{k,M+2} - h_{k,M}}{2h} = 0, \quad k = 0, 1, 2, ..., K.$$

The mesh point r_{M+2} is not in [0, 1] and so the values $f_{k,M+2}$, $h_{k,M+2}$ seem extraneous. However, they are eliminated by imposing the difference equations in (4.2) at $j = M + 1$. The results, after using (4.6b) and the above, is for $\varepsilon = 0$:

$$g_{k,M+1} = -\frac{2}{h^2} f_{k,M}, \quad k = 1, 2, ..., K, \tag{4.7a}$$
$$v_{k,M+1} = -\frac{2}{h^2} h_{k,M}, \quad k = 0, 1, 2, ..., K. \tag{4.7b}$$

For $\varepsilon > 0$ we must add the terms:

$\frac{1}{2}\varepsilon[g_{k-1,M+1} + g_{k+1,M+1} + D_+D_-(f_{k-1,M} + f_{k+1,M})]$ for (4.7a),

$\frac{1}{2}\varepsilon[v_{k-1,M+1} + v_{k+1,M+1} + D_+D_-(h_{k-1,M} + h_{k+1,M})]$ for (4.7b).

The numerical problem is to solve the nonlinear system of the difference equations in (4.2), (4.3), (4.4), (4.5), and (4.7). These form $6KM + 2K + 3M + 2$ equations. There are precisely that many unknowns $\{f_{k,j}, h_{k,j}, g_{k,j}, v_{k,j}, w_{k,j}, u_{k,j}\}$ when the quantities in (4.6) are eliminated. We go further and use (4.7) to eliminate the $2K + 1$ quantities $\{g_{k,M+1}, v_{k,M+1}\}$. Then we have only $(6K + 3)M + 1$ equations and unknowns.

TABLE I

Critical Dean Number F_m (m = 1, 2), Fold Points; B_1, Bifurcation Point

K	h	ε	F_1	F_2	B_1
10	$\frac{1}{40}$	0.0	12752.2	950.4	12734.0
10	$\frac{1}{40}$	0.05	12822.9	1036.0	12355.7
10	$\frac{1}{40}$	0.1	12963.2	1129.8	12026.4
15	$\frac{1}{40}$	0.0	12118.4	951.5	12111.6
15	$\frac{1}{40}$	0.05	11783.2	1025.9	11777.5
15	$\frac{1}{40}$	0.1	11491.6	1106.5	11484.0

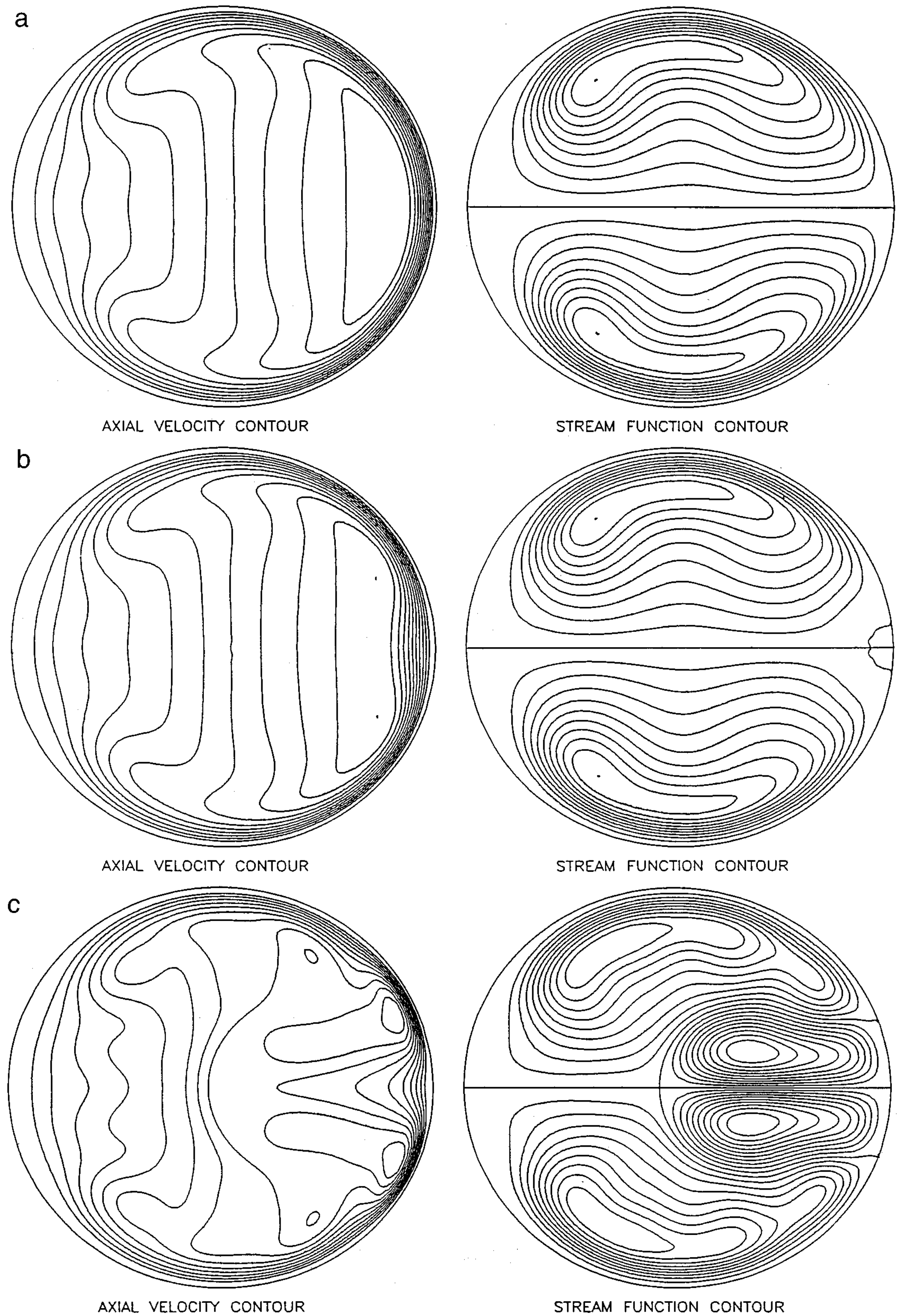

FIG. 6. Axial velocity, w, and stream function, ϕ, contour lines: $D = 8000$, $K = 10$, $h = \frac{1}{40}$, $\varepsilon = 0.1$. (a) First symmetric branch: Max $w = 622.3$, Min $w = 0$, Max $\phi = 22.4$, Min $\phi = -22.4$. (b) Second symmetric branch: Max $w = 631.5$, Min $w = 0$, Max $\phi = 21.52$, Min $\phi = -21.52$. (c) Third symmetric branch: Max $w = 606.9$, Min $w = 0$, Max $\phi = 20.81$, Min $\phi = -20.81$. (d) $D = 18000$. Asymmetric branch: Max $w = 1100$, Min $w = 0$, Max $\phi = 30.59$, Min $\phi = -30.59$.

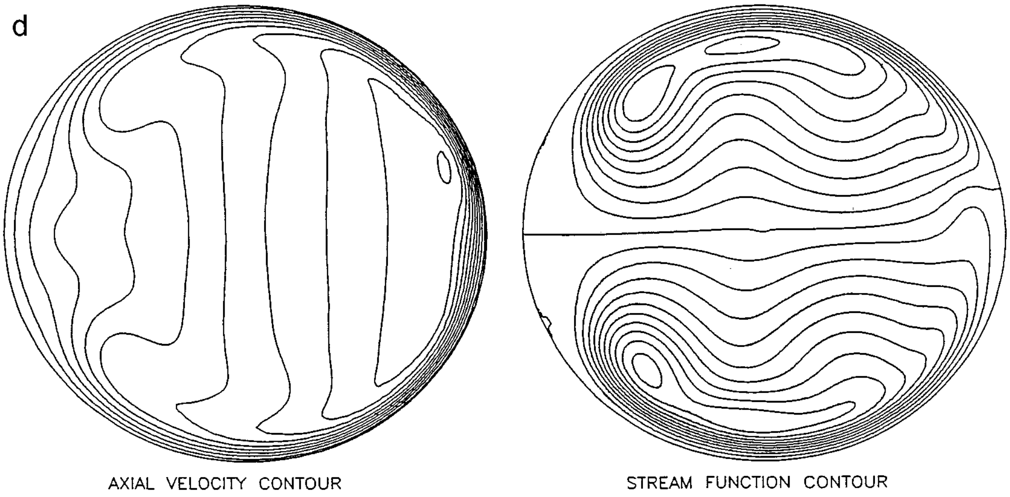

FIG. 6—*Continued*

4.3. *Newton's Method and Path Following Techniques*

To solve the difference equations we use Newton's method combined with continuation procedures to ensure good initial estimates of the solution as the parameters are varied. To do this efficiently the unknowns must be ordered in a manner that simplifies the structure of the Jacobian matrix. To describe our ordering we first introduce the vectors f_j, h_j, g_j, v_j, u_j, and w_j of dimensions K, $K + 1$, K, $K + 1$, K, and $K + 1$, respectively:

$$f_j^T \equiv (f_{1,j}, f_{2,j}, ..., f_{K,j}), \qquad 1 \le j \le M;$$
$$h_j^T \equiv (h_{0,j}, h_{1,j}, ..., h_{K,j}), \qquad 1 \le j \le M;$$
$$g_j^T \equiv (g_{1,j}, g_{2,j}, ..., g_{K,j}), \qquad 1 \le j \le M + 1;$$
$$v_j^T \equiv (v_{0,j}, v_{1,j}, ..., v_{K,j}), \qquad 1 \le j \le M + 1;$$
$$u_j^T \equiv (u_{1,j}, u_{2,j}, ..., u_{K,j}), \qquad 1 \le j \le M;$$
$$w_j^T \equiv (w_{0,j}, w_{1,j}, ..., w_{K,j}), \qquad 1 \le j \le M.$$

Recall that (4.7) gives $g_{M+1} = -2/h^2 f_M$ and $v_{M+1} = -2/h^2 h_M$ (for the case $\varepsilon = 0$). Therefore, g_{M+1} and v_{M+1} can be eliminated. The remaining $(6K + 3)M + 1$ unknowns are represented in the vector

$$X^T \equiv (w_{0,0}; f_1^T, g_1^T, u_1^T, h_1^T, v_1^T, w_1^T; ...; f_M^T, g_M^T, u_M^T, h_M^T, v_M^T, w_M^T). \tag{4.8}$$

Now we order the equations in a corresponding manner. That is, for a fixed j-value we take (4.5) and all of (4.2a) for $1 \le k \le K$, (4.2b) for $0 \le k \le K$, (4.3a), (4.3b) for $1 \le k \le K$, (4.4a) for $1 \le k \le K$, (4.4b) for $0 \le k \le K$. The equations ordered in this manner for $j = 1, 2, ..., M$ and finally (4.5) for $j = M + 1$ can be written as a vector equation in the form

$$G(X; D, \varepsilon) = 0. \tag{4.9}$$

We denote solutions of (4.9) by $X = X(D, \varepsilon)$. It is obvious that (4.9) has an exact solution $X(0, 0) = 0$. Newton's method and the continuation procedure are used to follow the solution branch of (4.9) for the case of regular $G_X(X(D, \varepsilon), D, \varepsilon)$. The initial estimation for $X(D + \delta D, \varepsilon)$ can be obtained by

$$X^{(0)}(D + \delta D, \varepsilon) = X(D, \varepsilon) + \delta D X_D(D, \varepsilon), \tag{4.10}$$

where $X_D(D, \varepsilon)$ satisfies

$$G_X(X(D, \varepsilon); D, \varepsilon) X_D(D, \varepsilon) = - G_D(X(D, \varepsilon); D, \varepsilon). \tag{4.11}$$

The iterative sequence $\{X^{(i)}(D + \delta D, \varepsilon)\}$ can be obtained by solving

$$\begin{aligned} G_X(X^{(i)}; D + \delta D, \varepsilon)(X^{(i+1)} - X^{(i)}) \\ = -G(X^{(i)}; D + \delta D, \varepsilon), \quad i = 0, 1, ... \end{aligned} \tag{4.12}$$

Here G_X is the Jacobian matrix which as a result of the above-indicated ordering has the block-banded structure shown below. Each square block is a submatrix of order $(6K + 3) \times (6K + 3)$.

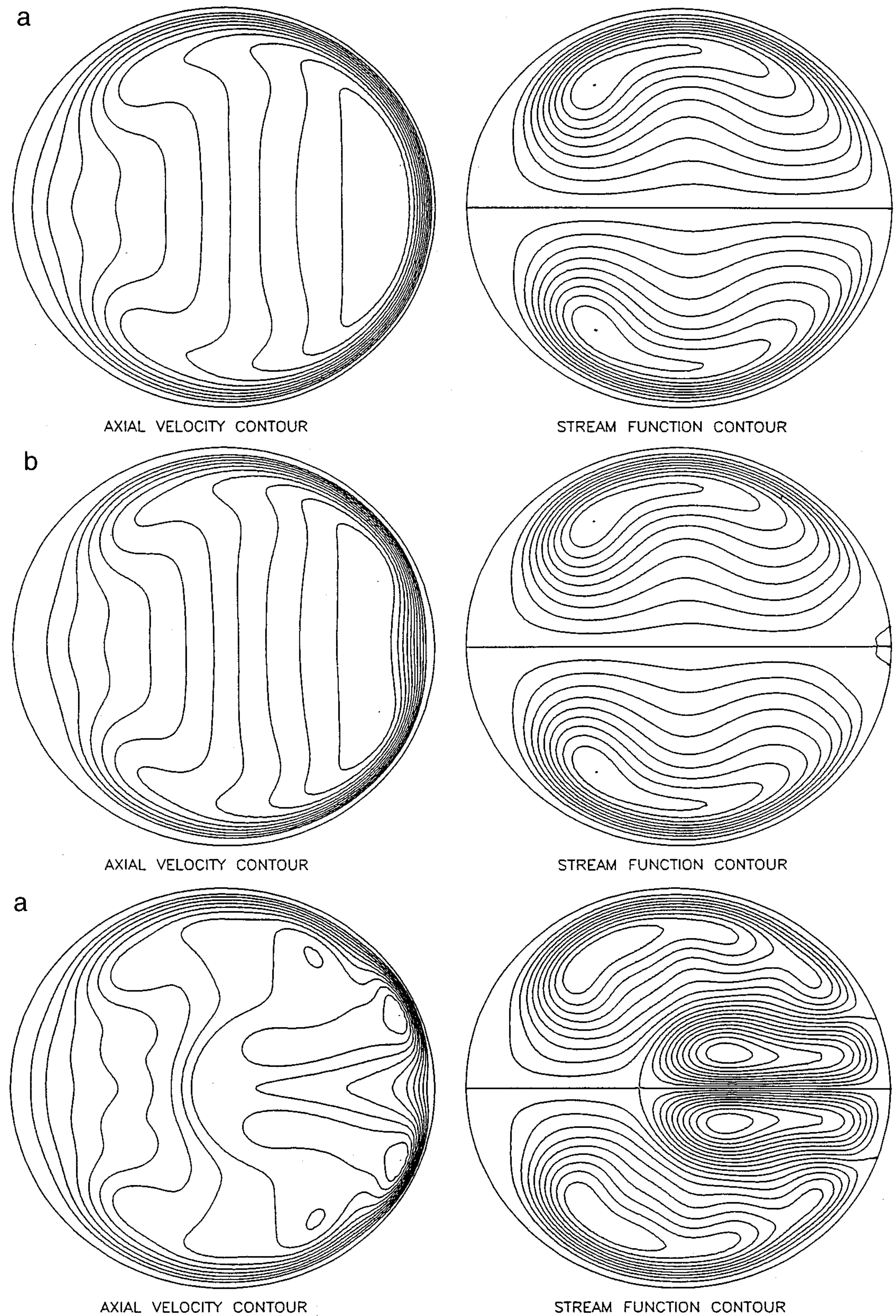

FIG. 7. Axial velocity, w, and stream function, ϕ, contour lines: $D = 8000$, $K = 15$, $h = \frac{1}{40}$, $\varepsilon = 0$. (a) First symmetric branch: Max $w = 621.8$, Min $w = 0$, Max $\phi = 23.95$, Min $\phi = -23.95$. (b) Second symmetric branch: Max $w = 632.5$, Min $w = 0$, Max $\phi = 22.93$, Min $\phi = -22.93$. (c) Third symmetric branch: Max $w = 598.1$, Min $w = 0$, Max $\phi = 21.69$, Min $\phi = -21.69$. (d) $D = 18000$. Asymmetric branch: Max $w = 1113$, Min $w = 0$, Max $\phi = 32.21$, Min $\phi = -32.21$.

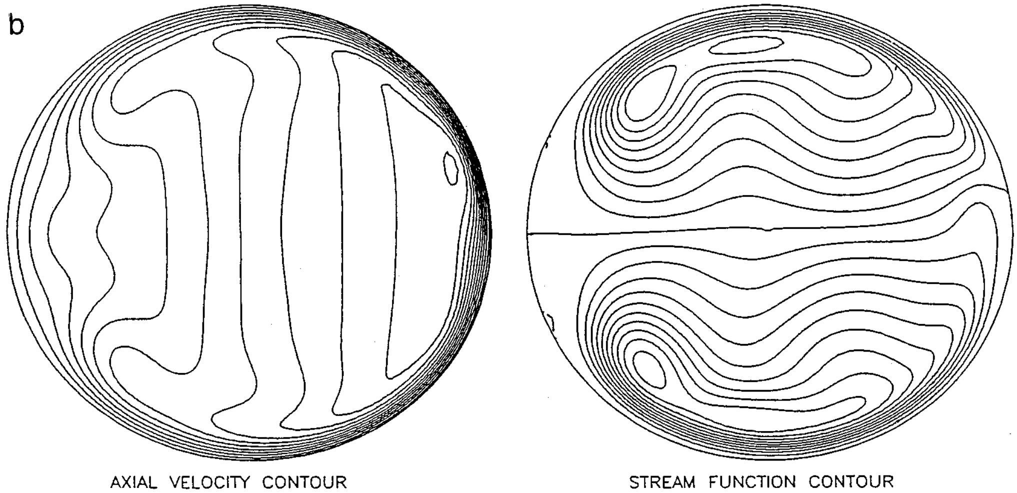

FIG. 7—*Continued*

$$G_X \equiv \begin{bmatrix} [\,] & [\quad] & & & & \\ [\,] & [\quad] & [\quad] & & & \\ & [\quad] & [\quad] & [\quad] & & \\ & & \ddots & \ddots & \ddots & \\ & & & [\quad] & [\quad] & [\quad] \\ & & & & [\quad] & [\quad] \end{bmatrix}.$$

There are M such rows of blocks. The matrix is block tridiagonal. All other elements in G_X are zero. Most of the computing effort goes into solving the linear algebraic systems in (4.12). Thus, we use (4.10) to get a good initial estimate to reduce the computational cost. The method described in (4.10)–(4.12) is known as Euler–Newton continuation. It is extremely effective and usually converges quadratically, except for the case of singular G_X. The failure of the method to converge does usually signal the presence of a bifurcation or fold point on the solution path being generated. In particular, a simple fold with respect to D is a singular solution, say (X^*, D^*), which has the properties that:

(1) dim $\mathrm{Null}(G_x^*) = 1$; i.e., all solutions of $G_X^*\phi = 0$ are $\phi \equiv \alpha\phi_0$, $\alpha \in R$, for some nontrival symmetric ϕ_0, That is, $0 \neq \phi \in X_S = \{x|Sx = x\}$.

(2) $G_D^* \notin \mathrm{Range}(G_X^*)$; i.e., $\langle\psi, G_D^*\rangle \neq 0$ for all solutions of $(G_X^*)^T\psi = 0$.

A symmetry-breaking bifurcation point with respect to D is a solution which has the property (1), except for $\phi \in X_a = \{x|Sx = -x\}$ and

(2)′ $G_D^* \in \mathrm{Range}(G_X^*)$; i.e., $\langle\psi, G_D^*\rangle = 0$, and

$$G_{DX}^*\phi + G_{XX}^*\phi v \notin \mathrm{Range}(G_X^*),$$

where $v \in X_s = \{x|Sx = x\}$ is uniquely determined by

$$G_X^* v + G_D^* = 0. \tag{4.13}$$

The group theory applied to the bifurcation problem shows that the solution path of (4.9) consists locally of two smooth transversally intersecting branch C_s (symmetric) and C_a (asymmetric) with the following representations (see [1]):

$$\begin{aligned} C_s = \{(X, D) : X &= X^* + \xi v + w_1(\xi), \\ D &= D^* + \xi, |\xi| < \delta_0\}, \end{aligned} \tag{4.14a}$$

$$\begin{aligned} C_a = \{(X, D) : X &= X^* + \xi\phi + w_2(\xi), \\ D &= D^* + \mathrm{O}(\xi^2), |\xi| < \delta_0\}, \end{aligned} \tag{4.14b}$$

where $\|w_i\| = O(\xi^2)$, $i = 1, 2$, $v \in X_s$, $\phi \in \mathrm{Null}(G_D^*) \cap X_a$, v is given by (4.13). The asymptotic expression (4.13) is useful for the initial estimate of the Newton's method which is very effective and quadratically convergent to follow the asymmetric solution branch near the symmetry-breaking bifurcation point.

To overcome the difficulty caused by the singularity, pseudo-arclength continuation is introduced as in [9]; that is, we do not parameterize the solution path by D, but rather introduce a new pseudo-arclength parameter s and a new scalar constraint and seek to solve the augmented system

$$G(X(s), D(s), \varepsilon) = 0, \tag{4.15a}$$

$$\begin{aligned} N(X(s), D(s), s) \equiv \langle \dot{X}(s_0), [X(s) - X(s_0)] \rangle \\ + \dot{D}(s_0)[D(s) - D(s_0)] \\ + (s - s_0) = 0. \end{aligned} \tag{4.15b}$$

Here $[X(s_0), D(s_0)]$ is a previously computed solution for ε fixed in the present discussion and for $s = s_0$. By $\dot{X} = dX/ds$, $\dot{D} = dD/ds$ we denote the components of a tangent vector to the solution path $\{X(s), D(s)\}$. The constraint simply requires that the point $(X(s), D(s))$ lies on the plane normal to this tangent at a distance $(s - s_0)$ from the point of tangency.

We use the system (4.15) when the previous Euler–Newton scheme begins to show signs of failure (i.e., too many iterations until convergence). We solve (4.14) by Newton's method. The Jacobian of this system is

$$\frac{\partial(G, N)}{\partial(X, D)} = \begin{pmatrix} G_X & G_D \\ N_X & N_D \end{pmatrix}, \tag{4.16}$$

where $N(X, D, s)$ is the left side of (4.14b). This Jacobian is nonsingular at the regular solution points and at the simple fold points. This is why our method has no difficulties in computing solution paths through folds. To solve for the Newton iterations, we use the bordering algorithm described in [7] which is designed for systems with coefficients as shown in (4.16).

4.4. *Stability*

The unsteady-state Navier–Stokes equations take the form

$$\frac{\partial w}{\partial \tau} = \tilde{\nabla}^2 w + \frac{1}{r(1 + \varepsilon r \cos\alpha)} \left(\frac{\partial \phi}{\partial r} \frac{\partial w}{\partial \alpha} - \frac{\partial \phi}{\partial \alpha} \frac{\partial w}{\partial r} \right) + D, \tag{4.17a}$$

$$\begin{aligned} \frac{\partial}{\partial \tau}(-\tilde{\nabla}^2 \phi) = -\tilde{\nabla}^4 \phi + \frac{1}{r(1 + \varepsilon r \cos\alpha)} \\ \left(\frac{\partial \phi}{\partial r} \frac{\partial}{\partial \alpha} - \frac{\partial \phi}{\partial \alpha} \frac{\partial}{\partial r} \right)(-\tilde{\nabla}^2 \phi) \\ + \frac{2\varepsilon(-\tilde{\nabla}^2 \phi)}{(1 + \varepsilon r \cos\alpha)^2} \left(\sin\alpha \frac{\partial \phi}{\partial r} + \frac{\cos\alpha}{r} \frac{\partial \phi}{\partial \alpha} \right) \\ - \frac{w}{(1 + \varepsilon r \cos\alpha)^2} \left(\sin\alpha \frac{\partial w}{\partial r} + \frac{\cos\alpha}{r} \frac{\partial w}{\partial \alpha} \right), \end{aligned} \tag{4.17b}$$

where time is scaled as $\tau = \nu t/a^2$.

After discrete approximations, the system equations can be written in the form as

$$\mathscr{A} \frac{\partial X}{\partial \tau} = \tilde{G}(X; D, \varepsilon),$$

where $\mathscr{A}$ is a positive definite matrix which is the approximation of the operator $\begin{pmatrix} I & 0 \\ 0 & -\tilde{\nabla}^2 \end{pmatrix}$, $\tilde{G}(X; D, \varepsilon)$ is the approximation of the right side of (4.17) which is equivalent to $G(X; D, \varepsilon)$.

The sign of eigenvalues of Jacobian $\mathscr{A}^{-1}\tilde{G}_X(X_0; D, \varepsilon)$, where X_0 denotes a steady-state solution, determines the stability of the flow. Since $\mathscr{A}^{-1}$ is also positive definite, the sign of the corresponding eigenvalues of $\mathscr{A}^{-1}\tilde{G}_X(X_0; D, \varepsilon)$ and $\tilde{G}_X(X_0; D, \varepsilon)$ is the same. During the computation, the appearance of the positive eigenvalues of $\tilde{G}_X(X_0; D, \varepsilon)$ is monitored (Fig. 2). The bifurcation analysis can also be made to decide the stability of the flows, because the bifurcation phenomena is connected with the change of the stability.

5. EXTENDED SYSTEMS

In order to locate the fold point and the symmetry-breaking bifurcation points accurately, an extended set of equations

$$\begin{aligned} G(X, D) = 0 \\ G_X(X, D)\phi = 0 \\ L\phi - 1 = 0 \end{aligned} \tag{5.1}$$

was proposed respectively by Moore and Spence [8], Werner and Spence [11] for detecting the fold point and the symmetry-breaking bifurcation point. Here $X \in X_s$, $\phi \in X_s$ for the fold point, $\phi \in X_a$ for the symmetry-breaking bifurcation point, and L is a linear functional which normalizes ϕ. The Jacobian matrix of (5.1) is

$$\begin{pmatrix} G_X & 0 & G_D \\ G_{XX}\phi & G_X & G_{XD}\phi \\ 0 & L & 0 \end{pmatrix} \tag{5.2}$$

which is regular at the fold point or the symmetry-breaking bifurcation point. The regularity of (5.2) implies that the Newton method can be used to solve (5.1). The effective algorithms were designed in [8, 11] to solve Newton's iterations with Jacobian (5.2).

6. NUMERICAL RESULTS AND DISCUSSION

In addition to the stream function and flow velocity, we have computed Re, the Reynolds number based on the mean axial velocity,

$$\mathrm{Re} = 2\sqrt{2}\int_0^1 w_0(r)rdr,$$

and the friction ratio (ratio of curved, γ_c, to straight, γ_s, wall friction):

$$\frac{\gamma_c}{\gamma_s} = 4\sqrt{2}\,\mathrm{Re}/D.$$

We have computed solution paths with D varying for the Fourier truncation $K = 10$, mesh spacing $h = 1/40$, and coiling ratio $\varepsilon = 0.0$. Starting from the trival state for $D = 0$ and $\varepsilon = 0.0$, we used continuation with D increasing as described in Section 4. A simple fold point F_1 was found and arclength continuation was used to accurately locate the fold point and traverse it. The solution branch was then continued with decreasing D and another fold point F_2 was found. Again, this fold was located accurately and traversed to obtain a third branch now with D increasing. From the results, we see that all these solution branches represent the symmetric flows. That is, all of $h_{k,j}$, $v_{k,j}$, $u_{k,j}$ are zero. The two fold points F_1 and F_2 are at $D = 12752.2$ and $D = 950.4$. These are in accordance with those computed in [13]. We refer to [13] for more details about the numerical results and discussions about the symmetric solution branches. Here we show in Fig. 5a–Fig. 5c plots of contour lines of the stream function and axial velocity for the symmetric solution at $D = 8000.0$. The graph of γ_c/γ_s vs D are given in Fig. 3.

After the first simple fold point was traversed, we found the signal that there exists another singular point which was not found in [13]. The extended system (5.1) was used to detect the symmetry-breaking bifurcation point B_1 which was found at $D = 12734.0$ near the first fold point. Then the asymptotic expression (4.14b) of the asymmetric branch was used for the initial estimate of the Newton's method, which is effective to follow the asymmetric branch. We could see the pattern of the asymmetric solution at $D = 18000.0$ in Fig. 5d. We have computed the asymmetric solution branch up to $D = 33000.0$, which is still disconnected with the symmetric solution branch, and no other bifurcation points have been found. The further computation will be needed to detect more structure of the solution path of the flows and the new symmetric solutions branch is expected to connect the asymmetric solution branch.

Similarly, we have also found the same solution structure for the following sets of values of Fourier truncation K, mesh spacing h, and the coiling ratio ε:

(i) $K = 10$, $h = \frac{1}{40}$; $\varepsilon = 0.05$, $\varepsilon = 0.1$.
(ii) $K = 15$, $h = \frac{1}{40}$; $\varepsilon = 0.0$, $\varepsilon = 0.05$, $\varepsilon = 0.1$.

The critical values of the Dean number are shown in Table I. The contours of the stream function and the axial velocity at $D = 8000.0$ for the symmetric solution and at $D = 18000.0$ for the asymmetric solution are shown in Fig. 6 and Fig. 7, corresponding to the case $K = 10$, $h = \frac{1}{40}$, $\varepsilon = 0.1$ and the case $K = 15$, $h = \frac{1}{40}$, $\varepsilon = 0.0$, respectively.

During the computation, we monitor the appearance of the positive eigenvalues of Jacobian $G_X(X; D, \varepsilon)$. The stability results are schematically shown in Fig. 2 for the case of $k = 10$, $h = \frac{1}{40}$.

Let M_p denote the number of positive eigenvalues of the Jacobian on the solution branches. $M_p = 0$ on OF_1 and $M_p \geq 1$ on the other branches, which means that only the symmetric two vortex flows on the solution branch OF_1 are stable to asymmetric disturbances and the other solution flows, including the asymmetric solution flows, are unstable.

REFERENCES

1. F. Brezzi, J. Rappaz, and P. Raviart, *Numer. Math.* **38,** 1 (1981).
2. W. M. Collins and S. C. R. Dennis, *Q. J. Mech. Appl. Math.* **28,** 133 (1975).
3. P. Daskopoulos and A. M. Lenhoff, *J. Fluid Mech.* **203,** 125 (1989).
4. W. R. Dean, *Philos. Mag.* **4,** 208 (1927).
5. W. R. Dean, *Philos. Mag.* **5,** 673 (1928).
6. S. C. R. Dennis, *J. Fluid Mech.* **99,** 449 (1980).
7. S. C. R. Dennis and M. Ng, *Q. J. Mech. Appl. Math.* **35,** 305 (1982).
8. G. Moore and A. Spence, *SIAM J. Numer. Anal.* **17,** 567 (1980).
9. H. B. Keller, "Numerical Solutions of Bifurcation and Nonlinear Eigenvalue Problems," in *Applications of Bifurcations Theory,* edited by Rabinowitz (Academic Press, New York, 1977), p. 359.
10. M. D. Van Dyke, *J. Fluid Mech.* **86,** 129 (1978).
11. B. Werner and A. Spence, *SIAM J. Numer. Anal.* **21,** 388 (1984).
12. K. H. Winters, *J. Fluid Mech.* **180,** 343 (1987).
13. Z. Yang and H. B. Keller, *Appl. Numer. Math.* **2,** 257 (1986).